Enzymatic Biodegradation of Poly(ethylene oxide-*b*-ϵ-caprolactone) Diblock Copolymer and Its Potential Biomedical Applications

Zhihua Gan,[†] Tsz Fung Jim,[†] Mei Li,[†] Zhao Yuer,[‡] Shenguo Wang,[§] and Chi Wu*[,†,‡]

Department of Chemistry, The Chinese University of Hong Kong, Shatin, N.T., Hong Kong; Department of Chemical Physics, The Open Laboratory of Bone-selective Chemistry, University of Science and Technology of China, Hefei, Anhui, China; and Laboratory of Membranes and Medical Polymers, Institute of Chemistry, Chinese Academy of Sciences, Beijing 100080, China

Received July 16, 1998; Revised Manuscript Received November 30, 1998

ABSTRACT: Water-insoluble poly(ethylene oxide-*b*-ϵ-caprolactone) (PEO-*b*-PCL) diblock copolymer (M_w = 1.71 × 10^4 g/mol and W_{PEO} = 20%) was successfully micronized into small polymeric core−shell nanoparticles (micelles) stable in water via a microphase inversion method. Such formed PEO-*b*-PCL nanoparticles are biodegradable in the presence of Lipase PS (enzyme). The biodegradation of the PEO-*b*-PCL nanoparticles, actually, only the hydrophobic PCL core, was monitored by laser light scattering. The biodegradation extent could be influenced by both the copolymer and enzyme concentrations, while the biodegradation rate was mainly determined by the enzyme concentration. Using pyrene as an imitative drug and fluorescence spectroscopy, we have shown that hydrophobic drugs can be easily loaded into the PCL core in the micronization process, and the biodegradation of the PCL block results in the dissolution of the nanoparticles and the releasing of pyrene molecules because the PEO block is soluble in water. The potential biomedical application of the PEO-*b*-PCL nanoparticles as a controlled release device has been demonstrated.

Introduction

Polymeric colloid particles have been widely used in biomedical applications. One typical example is drug delivery which can be either external or oral. In intravenous administration, one of the primary objectives is to design a device to deliver a drug to a specified site and release it at a proper rate. Narrowly distributed small polymeric nanoparticles in the size range 10−100 nm are ideal for intravenous injection because they are much smaller than the inner diameter (≥4 μm) of blood capillaries.[1] Consequently, polymeric nanoparticles can be used in sustained-release injection or as a target delivery to a specific organ. It has been shown that the irritant reaction at the injection site can be minimized by decreasing the particle size.[2]

Naturally, biodegradable and biocompatible polymer nanoparticles are of special interest. The commonly used biodegradable and biocompatible polymers are aliphatic polyesters, such as poly(lactic acid) (PLA), poly(glycolic acid) (PGA), poly(ϵ-caprolactone) (PCL) and their copolymers.[3,4] The nanoparticles made of these polymers can be directly absorbed by body or biodegraded into nonharmful products.[5,6] For a given type of polymer, the biodegradation rate and the releasing kinetics of loaded drugs can be adjusted by its chemical composition and molar mass.[7] The biomedical applications of polymeric nanoparticles have been extensively studied.[8−14] Different methods of preparing polymeric nanoparticles, such as the solvent evaporation and solvent displacement, have been reported.[15] Often, surfactants were used to stabilize the nanoparticles in aqueous solution because the aggregation and/or precipitation of water-insoluble polymers, such as PLA and PCL, would prevent many applications. Unfortunately, low molar mass surfactant molecules are sometimes harmful in biomedical applications.

On the other hand, extensive fundamental studies have shown that some block and graft copolymers could form polymeric micelles in selective solvents.[16−19] Amphiphilic block and/or graft copolymers with one poly(ethylene oxide) (PEO) block have attracted much attention because PEO has some unique properties, such as low protein adsorption and low cell adhesion.[20,21] It has been reported that hydrophobic therapeutic agents could be effectively encapsulated into the polymeric micelles.[22,23] Langer et al.[24,25] studied the structures and applications of the nanoparticles made of amphiphilic biodegradable block copolymers.

In this study, we have shown that the PEO-*b*-PCL diblock copolymer can be micronized into polymeric nanoparticles stable in aqueous solution without the help of any surfactant and studied the biodegradation of such formed PEO-*b*-PCL nanoparticles in the presence of Lipase PS (enzyme) on the basis of our previous investigation of the enzymatic biodegradation of PCL.[26] Using pyrene as an imitative drug and fluorescence spectroscopy, we have demonstrated that the PEO-*b*-PCL nanoparticles can be used as a potential biomaterial to make controlled releasing devices.

Experimental Section

Sample Preparation. The poly(ethylene oxide-*b*-ϵ-caprolactone) (PEO-*b*-PCP) block copolymer (M_w = 1.71 × 10^4 g/mol and W_{PEO} = 20%) was synthesized by sequential ring-opening polymerizations of ethylene oxide and ϵ-caprolactone monomers in the presence of (5,10,15,20-tetraphenylporphinato)-aluminum chloride as a catalyst.[27] Lipase PS (enzyme) from *Pseudomonas cepacia* (courtesy of Amano Pharmaceutical Co., Ltd., Nagoya, Japan) was further purified by freeze-drying. Pyrene as an imitative hydrophobic drug was used without purification. The micronization of the PEO-*b*-PCL block copolymer was made by adding 1 mL of tetrahydrofuran (THF) solution of PEO-*b*-PCL dropwise into 99 mL of deionized water

* To whom correspondence should be addressed.
[†] The Chinese University of Hong Kong.
[‡] University of Science and Technology of China.
[§] Chinese Academy of Sciences.

10.1021/ma981121a CCC: $18.00
Published on Web 01/21/1999

under ultrasonification. The initial copolymer concentration in THF was 10^{-3} g/mL. It is not hard to imagine that when one drop of the THF solution was added into an excess of water, THF was immediately mixed with water, and the water-insoluble PCL blocks started to aggregate to form small polymeric core−shell nanoparticles with the insoluble PCL blocks as the hydrophobic core and the soluble PEO blocks as the hydrophilic shell. The final copolymer concentration in the dispersion was 10^{-5} g/mL. The small amount of THF (1%) in the dispersion was removed under low pressure, and the resultant dispersion was transparent.

Laser Light Scattering (LLS). A modified commercial LLS spectrometer (ALV/SP-125) equipped with an ALV-5000 multi-τ digital time correlator and a solid-state laser (ADLAS DPY425II, out power = ~400 mV at λ = 532 nm) was used. In static LLS, the angular dependence of the excess absolute time-average scattered intensity, i.e., Rayleigh ratio $R_{vv}(q)$, was measured. For a dilute polymer solution at a relatively small scattering angle θ, $R_{vv}(q)$ can be related to the weight-average molar mass M_w, the second virial coefficient A_2, and the root-mean square z-average radius $\langle R_g^2\rangle_z^{1/2}$ (or simply as $\langle R_g\rangle$) by[28]

$$\frac{KC}{R_{vv}(q)} \approx \frac{1}{M_w}\left(1 + \frac{1}{3}\langle R_g^2\rangle_z q^2\right) + 2A_2C \qquad (1)$$

where $K = 4\pi^2(dn/dc)^2n^2/(N_A\lambda_0^4)$ and $q = (4\pi n/\lambda_0)\sin(\theta/2)$ with N_A, dn/dc, n, and λ_0 being Avogadro's number, the specific refractive index increment, the solvent refractive index, and the wavelength of light in a vacuum, respectively. At $q \to 0$ and $C \to 0$, $R_{vv}(q) \approx KCM_w$. In dynamic LLS, the intensity−intensity time correlation function $G^{(2)}(t,q)$ in the self-beating mode was measured.[28] The analysis of $G^{(2)}(t,q)$ could lead to the line-width distribution $G(\Gamma)$.[29] For a pure diffusive relaxation, Γ is related to the translational diffusion coefficient D by $\Gamma/q^2 = D$ at $C \to 0$ and $q \to 0$. In this case, $G(\Gamma)$ can be directly converted to a translational diffusion coefficient distribution $G(D)$ or a hydrodynamic radius distribution $f(R_h)$ by using the Stocks−Einstein equation: $R_h = k_BT/(6\pi\eta D)$ with k_B, T, and η being the Boltzmann constant, the absolute temperature, and the solvent viscosity, respectively.

Enzymatic Biodegradation. The biodegradation was in situ conducted inside the LLS cuvette. The PEO-*b*-PCL nanoparticle dispersion and the Lipase PS aqueous solution were respectively clarified by 0.45 and 0.5 μm Millipore filters. In a typical experiment, a proper amount of dust-free Lipase PS aqueous solution was directly added into 2 mL of dust-free PEO-*b*-PCL dispersion to start the biodegradation. Both $R_{vv}(q)$ and $G^{(2)}(t,q)$ were recorded during the enzymatic biodegradation.

Fluorescence Measurement. Both pyrene and the PEO-*b*-PCL block copolymers were completely soluble in THF. The initial copolymer and pyrene concentrations were ~10^{-3} and ~10^{-5} g/mL, respectively. The nanoparticles were prepared by the same micronization procedure used for the LLS experiments. THF was removed by evaporation. Since pyrene has a very low solubility in water, it is expected that in the microphase inversion nearly all pyrene molecules were encapsulated (trapped) inside the hydrophobic PCL core. The releasing of pyrene from the PEO-*b*-PCL nanoparticles was followed in terms of the fluorescence intensity change recorded by using a fluorescence spectrophotometer (model F-4500, Japan). In each measurement, 2 mL of PEO-*b*-PCL nanoparticle dispersion loaded with pyrene was placed in a 10 mm × 10 mm square quartz cell. The excitation wavelength λ_{ex} selected was 335 nm. The widths of the excitation and emission slits were 10 and 2.5 nm, respectively.

Results and Discussion

Figures 1 and 2 respectively show static and dynamic characterization of the PEO-*b*-PCL nanoparticles. The hydrodynamic radius distributions $f(R_h)$ in Figure 1 reveal that the PEO-*b*-PCL nanoparticles are narrowly distributed and have an average hydrodynamic radius

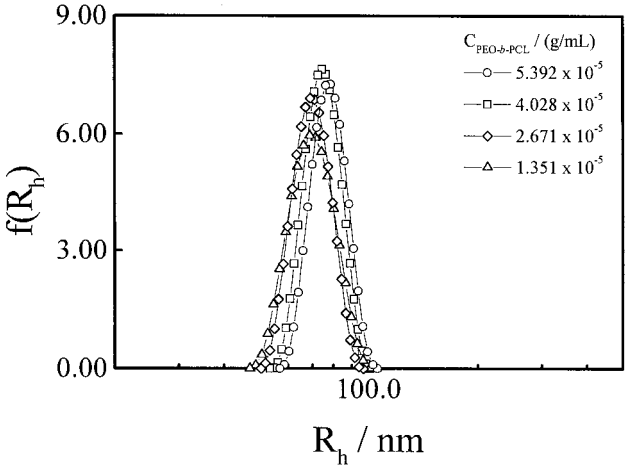

Figure 1. Concentration independence of the hydrodynamic radius distribution of the PEO-*b*-PCL nanoparticles in aqueous solution at 25 °C.

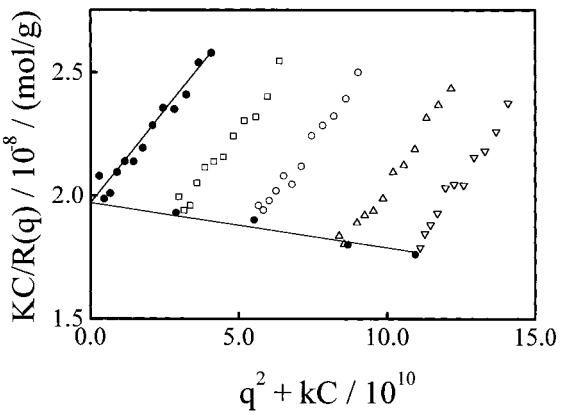

Figure 2. Typical Zimm plot of the PEO-*b*-PCL nanoparticles in aqueous solution at 25 °C, where C ranges from 1.351 × 10^{-5} to 5.392 × 10^{-5} g/mL.

Table 1. Characterization of the PEO-*b*-PCL Copolymer Chains and Nanoparticles at 25 °C

	solvent	molar mass	$\langle R_g\rangle$/ nm	A_2/ mol cm^3/g^2	$\langle R_h\rangle$/ nm
PEO-*b*-PCL chain	THF	1.71×10^4			10.9
PEO-*b*-PCL nanoparticles	H_2O	5.05×10^7	57.1	-1.84×10^{-5}	77.2

$\langle R_h\rangle$ of 77 nm. According to eq 1, the extrapolation of $[KC/R_{vv}(q)]_{C\to0,q\to0}$, the slopes of $[KC/R_{vv}(q)]_{C\to0}$ vs q^2, and $[KC/R_{vv}(q)]_{q\to0}$ vs C in Figure 2 respectively lead to M_w, $\langle R_g\rangle$, and A_2. The results are summarized in Table 1. The negative A_2 is expected because the PCL block is insoluble in water. The ratio of $\langle R_g\rangle/\langle R_h\rangle \sim 0.74$ indicates that the PEO-*b*-PCL nanoparticles are spherical. Using the results in Table 1, we estimate that, on average, each PEO-*b*-PCL nanoparticles contains ~3000 PEO-*b*-PCL chains and each PEO-*b*-PCL chains occupies a surface area of ~25 nm^2. Using $\langle\rho\rangle = M_w/(4\pi\langle R_h\rangle^2/3)$, we also estimated the average density $\langle\rho\rangle$ of the PEO-*b*-PCL chains before and after the microphase inversion to be 0.0035 and 0.045 g/cm^3, respectively. It is clear that even $\langle\rho\rangle$ increases more than 10-fold; the average density of the PEO-*b*-PCL nanoparticles is still much less than the density (~1 g/cm^3) of bulk PEO-*b*-PCL copolymer, indicating that the PEO-*b*-PCL nanoparticles were swollen, probably due to the stretching of the PEO blocks in the shell.

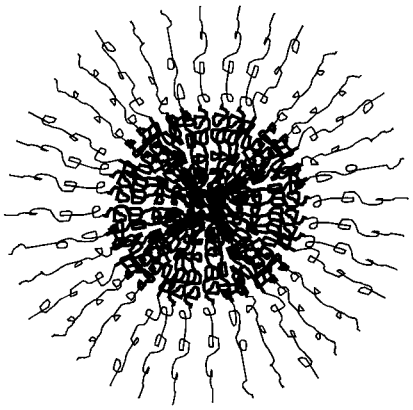

Figure 3. Schematic of the PEO-*b*-PCL core−shell polymeric nanoparticles.

Figure 3 shows a schematic of the PEO-*b*-PCL nanoparticle. The core−shell nanostructure resembles the micelle made of low molar mass surfactant molecules. It should be noted that, just as in the case of low molar mass surfactant, the onset of the intermolecular association of block or graft copolymers in a selective solvent can also be defined as critical micelle concentration (cmc) below which the copolymers exist as individual chains (unimer). When the copolymer concentration is higher than its cmc, the copolymer micelles are in a dynamic equilibrium with the unimers. In comparison with low molar mass surfactant molecules, block copolymers usually have a much lower cmc which is often imperceptible.[16] Our LLS results showed that the PEO-*b*-PCL copolymer has a cmc lower than 10^{-7} g/mL. Therefore, in the present study, the intensity of the light scattered from the unimer and enzyme can be ignored in comparison with that from the PEO-*b*-PCL nanoparticles.

Previously, we found that a combination of the enzymatic hydrolysis with the micronization not only greatly speeded up the biodegradation of PCL but also allowed us to follow the biodegradation kinetics by using laser light scattering.[26] In this study, we also found the average hydrodynamic radius $\langle R_h \rangle$ of the nanoparticles to be a constant during the biodegradation, indicating that the molar mass of the remaining PEO-*b*-PCL nanoparticles was a constant. Therefore, on the basis of eq 1, we know that the decrease of $R_{vv}(q)$ is only related to the decrease of the copolymer concentration C, i.e., $R_{vv}(q) \propto C$, so that $C_t/C_0 = [R_{vv}(q)]_t/[R_{vv}(q)]_0$. Figure 4 shows the enzyme concentration (E) dependence of the biodegradation of the PEO-*b*-PCL nanoparticles, where C_0 is the initial copolymer concentration, and the subscripts "0" and "t" represent $t = 0$ and $t = t$, respectively. In Figure 4, the initial slope leads to the initial biodegradation rate (v_0) defined as $[dC_t/dt]_{t\to 0}$. The inset shows the enzyme concentration dependence of v_0 and the line represents a least-squares fitting of v_0 (g/mL.min) $= 6.327 \times 10^{-5}E_0 2.0 \pm 0.1$. However, we still do not understand why v_0 is much dependent on the enzyme concentration E by the second order.

On the other hand, Figure 5 shows that, for a given Lipase PS concentration E_0, the biodegradation rate is nearly a constant, independent of the initial copolymer concentration C_0. As shown in a previous paper,[26] the biodegradation of PCL in the presence of enzyme involves the adsorption of enzymes onto the nanoparticles and the enzymatic hydrolysis of the PCL chains. At this moment, we do not know a detailed degradation

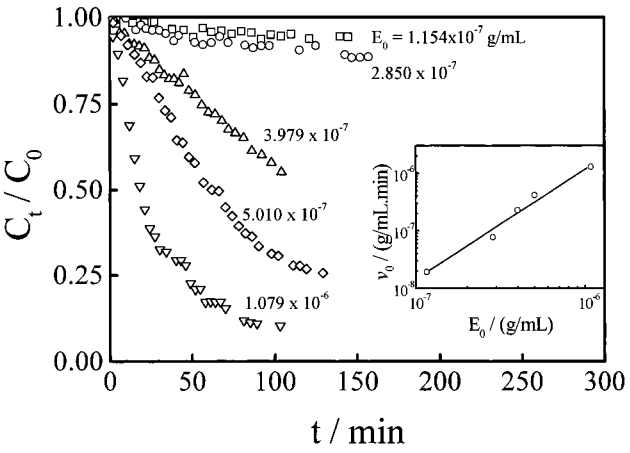

Figure 4. Enzyme concentration dependence of the biodegradation kinetics of the PEO-*b*-PCL nanoparticles at 25 °C, where $C_0 = 5.392 \times 10^{-3}$ g/mL and the inset shows the enzyme concentration dependence of the initial biodegradation rate (v_0).

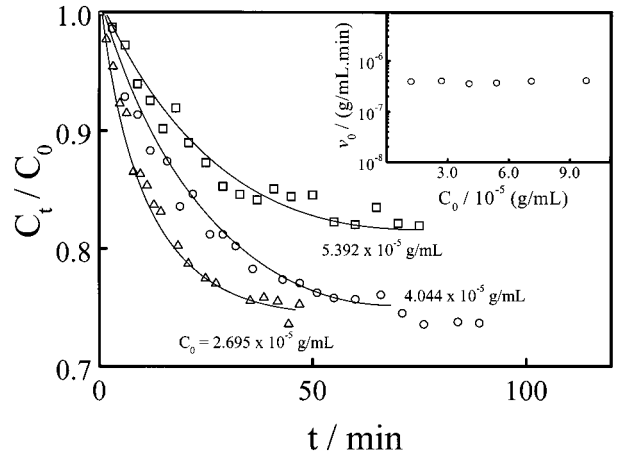

Figure 5. Copolymer concentration dependence of the biodegradation kinetics of the PEO-*b*-PCL nanoparticles at 25 °C, where $E_0 = 4.905 \times 10^{-7}$ g/mL and the inset shows the copolymer concentration dependence of the initial biodegradation rate (v_0).

mechanism but qualitatively know that the degradation of individual nanoparticles is fast as long as the hydrolysis starts and the nanoparticles were "eaten" by Lipase PS in a one-by-one fashion. For a given polymer concentration, more enzyme molecules can "eat" more nanoparticles per unit time, so that the biodegradation rate is mainly determined by the enzyme concentration. The results in Figure 5 once again suggest that the biodegradation of the PEO-*b*-PCL nanoparticles follows the one-by-one fashion.

Figures 4 and 5 reveal that the biodegradation rate of the PEO-*b*-PCL nanoparticles can be well controlled by both the copolymer and enzyme concentrations. Therefore, we thought that the PEO-*b*-PCL nanoparticles could be used as a potential controlled drug delivery device because hydrophobic drugs could be loaded into the PCL core and the biodegradation of the PCL core would lead to the dissolution of the PEO-*b*-PCL nanoparticles, resulting in a drug releasing. To test this idea, pyrene was chosen as an imitative drug because of its unique fluorescence characters and other properties. It is hydrophobic and has a very low solubility in water (7×10^{-7} M). Pyrene is preferentially solubilized into the hydrophobic region or microphase. When its environment changes from a polar to a

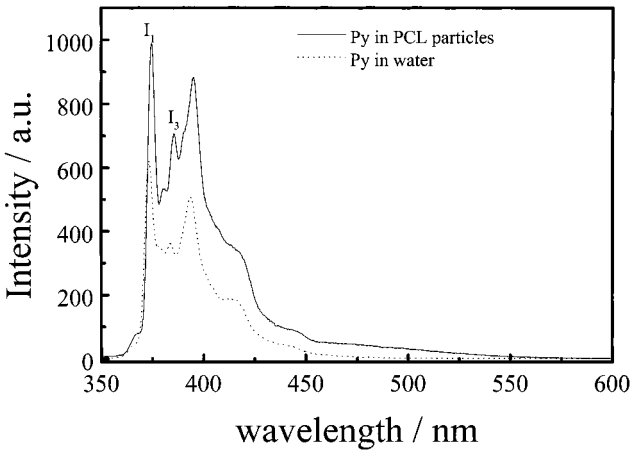

Figure 6. Fluorescence spectra of pyrene in pure water and in the presence of the PEO-*b*-PCL nanoparticles at 25 °C, where the copolymer and pyrene concentrations were 5.39 × 10^{-5} g/mL and 6 × 10^{-7} M, respectively.

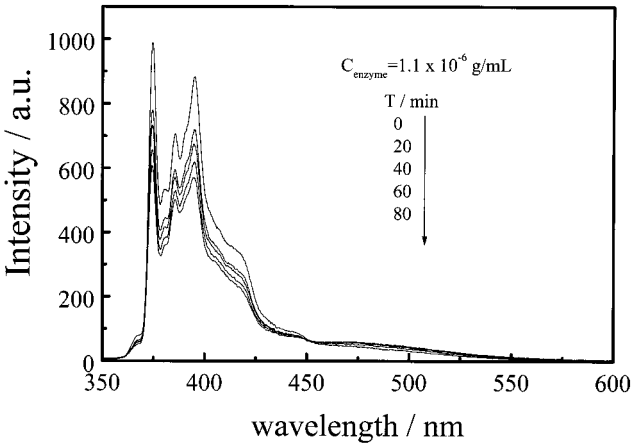

Figure 7. Fluorescence spectra of pyrene in the presence of the PEO-*b*-PCL nanoparticles during the biodegradation. For comparison, we also plot the fluorescence spectrum of pyrene in pure water (the dotted line at the bottom).

nonpolar one, there is a remarkable change in its emission spectra, such as an increase in the quantum yield and a decrease in its intensity ratio (I_1/I_3) of the first and third highest emission peaks. The ratio can change from ∼1.8 in water to ∼1.0 in the presence of anionic surfactant micelles or even lower values (∼0.6) in organic solvents.[30,31] Thus, the ratio can be used as an indicator of where pyrene is located.

Figure 6 shows the fluorescence spectra of pyrene free in pure water and in the presence of the PEO-*b*-PCL nanoparticles, where the copolymer and pyrene concentrations were 5.39 × 10^{-5} g/mL and 6 × 10^{-7} M, respectively. The pyrene concentration is lower than its saturated concentration in water in order to prevent the formation of microcrystals. Pyrene in water has a lower fluorescence intensity because of its short lifetime (200 ns) and low quantum yield. In the presence of the nanoparticles, pyrene shows a higher intensity, indicating that pyrene was loaded into the hydrophobic PCL core because pyrene has a longer lifetime (∼400 ns) and a higher quantum yield in a nonpolar environment.[32] In Figure 6, the intensity ratio (I_1/I_3) for pyrene in water is 1.75, close to the literature value. However, the ratio for pyrene in the presence of the nanoparticles is ∼1.4, higher than the expected values in a hydrophobic environment, which can be attributed to the low polymer concentration (∼5 × 10^{-5} g/mL) and the polar surface of PCE micelles.[31]

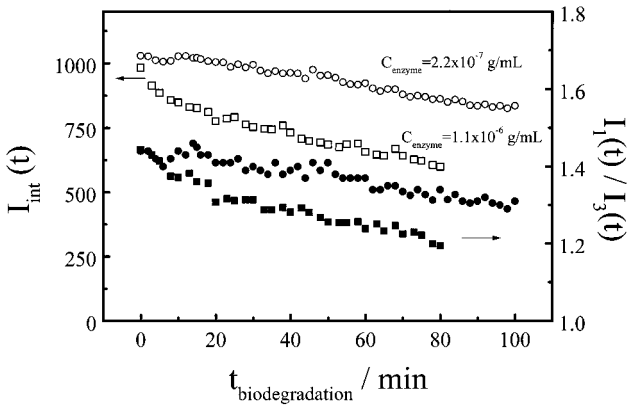

Figure 8. Biodegradation time dependence of the fluorescence intensity and the intensity ratio I_1/I_3 of pyrene in the presence of the PEO-*b*-PCL nanoparticles during the enzymatic biodegradation × 10^{-5} g/mL.

Figure 7 shows that the fluorescence intensity gradually decreases as the biodegradation time increases. Note that the enzyme had no effect on the fluorescence intensity for pyrene free in pure water. Hence, the decrease of the intensity is related to the release of pyrene from a less polar PCL core to water. This agrees well with the LLS results; namely, the scattering light intensity decreases during the biodegradation.

Figure 8 shows the time dependence of the fluorescence intensity and the intensity ratio I_1/I_3 of pyrene during the biodegradation. The decrease of the intensity ratio I_1/I_3 during the biodegradation is a surprise, which indicates the overall polarity of the environment decreases. One of the possible explanations is that the biodegradation produces a lot of small aliphatic acids which have a relatively low polarity in comparison with that of water. Figure 8 also shows that the decrease of the fluorescence intensity is a linear function of the biodegradation time and becomes fast when the enzyme concentration is higher.

In summary, the PEO-*b*-PCL block copolymer (M_w = 1.71 × 10^4 g/mol and W_{PEO} = 0.2) can be micronized into small narrowly distributed core−shell nanoparticles stable in water via a microphase inversion method. Such formed nanoparticles were biodegradable in the presence of Lipase PS (enzyme). The biodegradation extent can be influenced by both the copolymer and enzyme concentrations, and the biodegradation rate is mainly determined by the enzyme concentration. Using pyrene as an imitative drug, we have shown that hydrophobic drugs could be loaded into the hydrophobic PCL core, and the controllable biodegradation makes the PEO-*b*-PCL nanoparticles a potential biomedical material for the controlled releasing of hydrophobic drugs. Further studies in this direction are under way.

Acknowledgment. The financial support of the Research Grants Council of the Hong Kong Government Earmarked Grant 1997/98 (CUHK4181/97P, 2160082) and The National Natural Science Fundation, National Distinguished Young Investigator Fund (1996, 29625410) is gratefully acknowledged.

References and Notes

(1) Thews, G.; Mutschler, E.; Vaupel, P. *Anatomie, Physiologie, Pathophysiologie des Menschen*; Wissenschaftl, Verlagsges: Stuttgart, 1980; p 229.

(2) Little, K.; Parkhouse, J. *Lancet* **1962**, *2*, 857.
(3) Lewis, D. H. In *Biodegradable Polymers as Drug Delivery Systems*; Chassin, M., Langer, R., Eds.; Marcel Dekker: New York, 1990; pp 1−41.
(4) Peppas, L. B. *Int. J. Pharm.* **1995**, *116*, 1.
(5) Schindler, A. *Contemp. Top. Polym. Sci.* **1977**, *2*, 251.
(6) Kelly, R. J. *Rev. Surg.* **1970**, *2*, 142.
(7) Wagner, E.; Zenke, M.; Cotten, M.; Beug, H.; Birnstiel, M. L. *Proc. Natl. Acad. Sci. U.S.A.* **1990**, *87*, 3410.
(8) Kreuter, J. M. In *Microcapsules and Nanoparticles in Medicine and Pharmacy*; Donbrow, M., Ed.; CRC Press: Boca Raton, FL, 1992; pp 126−143.
(9) Allemann, E.; Doelker, E.; Gurny, R. *J. Pharm. Biopharm.* **1993**, *39*, 13.
(10) Fessi, H.; Puisieux, F.; Devissaguet, J. P.; Benita, S. *Int. J. Pharm.* **1989**, *55*, R1.
(11) Scholas, P. D.; Coombes, A. G. G.; Illum, L.; Davis, S. S.; Vert, M.; Davis, M. C. *J. Controlled Release* **1993**, *25*, 145.
(12) Molpeceres, J.; Guzman, M.; Aberturas, M. R.; Chacon, M.; Berges, L. *J. Pharm. Sci.* **1996**, *85*, 206.
(13) Chacon, M.; Berges, L.; Molpereres, J.; Aberturas, M. R.; Guzman, M. *Int. J. Pharm.* **1996**, *141*, 81.
(14) Lemoine, D.; Francois, C.; Kedzierwicz, F.; Preat, V.; Hoffman, M.; Maincent, P. *Biomaterials* **1996**, *17*, 2191.
(15) Song, C. X.; Labhasetwar, V.; Murphy, H.; Qu, X.; Humphrey, W. R.; Schebuski, R. J.; Levy, R. J. *J. Controlled Release* **1997**, *43*, 197.
(16) Tuzer, Z.; Kratochvil, P. In *Surface and Colloid Science*; Plenum Press: New York, 1993; Vol. 15, pp 1−83.
(17) Chu, B. *Langmuir* **1995**, *11*, 414.
(18) Xu, R.; Winnik, M. *Macromolecules* **1991**, *24*, 87.
(19) Liu, T.; Zhou, Z.; Wu, C.; Chu, B.; Schneider, D. K.; Nace, V. M. *J. Phys. Chem. B* **1997**, *101*, 8808.
(20) Hermans, I. *J. Chem. Phys.* **1982**, *77*, 2193.
(21) Dolan, A. K.; Edwards, S. F. *Proc. R. Soc. London* **1975**, *343*, 427.
(22) Alexandridis, P. *Colloid Interface Sci.* **1996**, *1*, 490.
(23) Chiu, H. C.; Chern, C. S.; Lee, C. K.; Chang, H. F. *Polymer* **1998**, *39*, 1609.
(24) Gref, R.; Minamitake, Y.; Peracchia, M. T.; Trubetskov, V.; Torchilin, V.; Langer, R. *Science* **1994**, *263*, 1600.
(25) Hrkach, J. S.; Peracchia, M. T.; Domb, A.; Langer, R. *Biomaterials* **1997**, *18*, 27.
(26) Gan, Z.; Jim, T. F.; Wu, C. *Polymer* **1999**, *40*, 1961.
(27) Gan, Z.; Jiang, B.; Zhang, J. *J. Appl. Polym. Sci.* **1996**, *59*, 961.
(28) Chu, B. *Laser Light Scattering*, 2nd ed.; Academic Press: New York, 1991.
(29) Berne, B.; Pecora, R. *Dynamic Light Scattering*; Plenum Press: New York, 1976.
(30) Kalyanasumdaram, K.; Thomas, J. K. *J. Am. Chem. Soc.* **1977**, *99*, 2039.
(31) Manfred, W.; Zhao, C.; Wang, Y.; Xu, R.; Winnik, M. *Macromolecules* **1991**, *24*, 1033.
(32) Kalyanasumdaram, K. *Langmuir* **1988**, *41*, 942.

MA981121A